J. Fluid Mech. (2003), *vol.* 494, *pp.* 285–296. © 2003 Cambridge University Press
DOI: 10.1017/S0022112003005834 Printed in the United Kingdom

Filling a collapsible tube

By JOSE-MARIA FULLANA[1], FRANÇOIS CROS[1], PATRICE FLAUD[2] AND STÉPHANE ZALESKI[3]

[1]Laboratoires Innothéra, 7-9 Avenue Francois-Vincent Raspail, 91110 Arcueil, France

[2]Laboratoire de Biorhéologie et d'Hydrodynamique Physicochimique, CNRS, Université René Diderot (Paris 7), France

[3]Laboratoire de Modélisation en Mécanique, CNRS, Université Pierre et Marie Curie (Paris 6), France
Jose-Maria.Fullana@Innothera.com

(Received 27 March 2003 and in revised form 9 July 2003)

We investigate experimentally and numerically the filling of a collapsible tube, motivated by venous hemodynamics in the lower limbs. The experiments are performed by filling an initially collapsed flexible tube, applying pressure through a hydraulic circuit. The tube law and the tube tension have been previously measured. The tube shape, the flow rate and the pressure at the two ends of the tube are measured continuously. The filling occurs in three stages: a rapid equilibration of the pressure near the tube entry with atmospheric pressure, a quasi-steady filling of the tube with a linearly rising pressure, and a final stage of tube inflation. Our numerical model is the classical one-dimensional collapsible tube equations. Excellent quantitative agreement is found between computations and experimental data. We show experimentally observed shapes near the tube end that indicate possible three-dimensional effects; however these effects do not impair significantly the ability of the one-dimensional model to describe the experiment. Travelling waves of large amplitude are observed in the simulations and the experiments.

1. Introduction

In this article, we investigate the filling of an elastic, collapsible tube with a liquid. The filling is a time-dependent process, which we investigate through laboratory experiments and two theoretical models. Our aim is a better understanding of blood flow in veins. The problem of fluid flow in biological vessels in general is complicated by the elasticity of the vessel walls. Many studies have been devoted to flow in arteries, airways or veins (Pedley 1980; Fung 1993). Veins are sometimes very deformable, to the point where they may collapse to almost vanishing cross-section. Venous flow is an important aspect of human physiology, as the orthostatic posture in humans creates a large pressure difference between the heart and the tip of the lower limbs. The pressure exerted by the heart is not sufficient to ensure an efficient circulation of the blood in these limbs. Thus a second mechanism occurs in healthy human physiology, in which the action of the muscles of the calves helps to periodically drain and fill the internal veins; it is called the muscular pump of the calf and is important as it reduces the internal vein pressure at the extremity of the legs. When it ceases to function, various pathologies, such as oedema and varicose veins may occur.

Here we focus on an idealized process of vein filling. The initial state of our flexible tube is entirely collapsed, with very low pressure. After opening of an external

https://doi.org/10.1017/S0022112003005834 Published online by Cambridge University Press

hydraulic line, the tube starts filling and we observe the corresponding dynamics. We also investigate a one-dimensional theoretical model of a collapsible tube. This model is integrated numerically and the results are compared with the experiment. This provides us with precise experimental data and a quantitative comparison with the theory of collapsible tubes, which is a first step in the understanding of the full physiological process of vein filling and draining. For instance, sudden postural changes from a lying to a standing position lead to rapid filling of the veins.

There have been numerous studies of flow in elastic and collapsible tubes, with applications to flows through arteries, veins, bronchi or urethrae (Griffiths 1971; Young & Tsai 1975; McClurken *et al.* 1981; Jan, Kamm & Shapiro 1983; Elad, Kamm & Shapiro 1987; Kamm & Pedley 1989). Many authors have proposed one-dimensional flow equations coupling elastic and fluid mechanical effects. These equations display a critical flow regime, when the flow velocity equals the velocity of wavy perturbations of large wavelength (Shapiro 1977). Phenomena such as flow limitation in Starling resistors (Conrad 1969; Holt 1969), and transition between supercritical and subcritical flow have been observed. Most experiments reproduce the setup of the Starling heart-lung machine: an horizontal tube with a supercritical section. For this case, many articles, e.g. Jensen & Pedley (1989), Jensen (1990, 1992), study the self-oscillations of the system in- steady in and outflow conditions. Other papers study the influence of space- and time-varying external pressure (Kamm & Shapiro 1979; Kamm 1982; Olson, Kamm & Shapiro 1982). The effect of longitudinal tension was studied in Pedley (1992). For Reynolds numbers of physiological interest Young & Tsai (1975) measured the pressure drop through constricted tubes, and Matsuzaki & Fung (1976, 1977) studied the separation phenomenon in two-dimensional channels. The situation where flow separates near a constriction was studied numerically by Cancelli & Pedley (1985), Matsuzaki & Matsumoto (1989) and Ikeda & Matsuzaki (1999). In Cancelli & Pedley (1985) flow separation is modelled by a step change in the nonlinear momentum advection term of the equations.

In contrast, our experiment involves a vertical tube filled with water in which gravity plays an important role, and flow is always subcritical. The external pressure is constant. On the other hand the in- or outflow is strongly time dependent. Thus a marked difference with the previous work is the study of the filling or draining effects, and the detailed comparison with experiment.

Our objective is to cross-validate experimental and numerical work. The detailed quantitative comparisons show that effects not incorporated in the models, such as three-dimensional effects near the ends of the tube, have little influence on the quantitative results.

2. Experimental setup and results

The hydrodynamic bench is depicted in figure 1. It is composed of a flexible tube (1) maintained in a vertical position by its ends. It is fixed on two rigid brass pipes (2 and 3) of larger diameter and its section was maintained slightly elliptic in order to force collapses in the double-lobe mode. It is known (Flaherty, Keller & Rubinow 1972) that the post-buckling behaviour of a uniform circular tube has a non-trivial solution for any negative value of the transmural pressure and for some $n > 2$ where n is the number of lobes.

The end position of the flexible tube is adjustable in height, giving the possibility of varying the tube tension. Two pressure sensors (at the top and bottom) measure the temporal variations of the pressure. The upper brass pipe is closed at the top.

https://doi.org/10.1017/S0022112003005834 Published online by Cambridge University Press

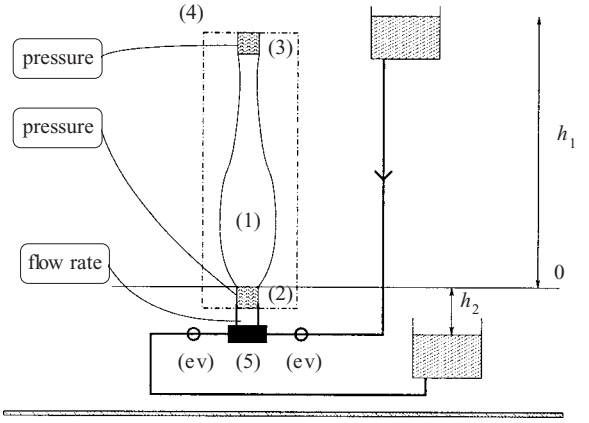


FIGURE 1. The hydrodynamic bench.

The lower brass pipe is part of a hydrodynamic circuit designed to carry the fluid upon filling and draining. This circuit contains two tanks in which a constant water level is maintained. This level is adjustable to provide the desired hydraulic charge. The circuit may be switched to the high-level tank for filling or the low-level tank for draining experiments. At the exit of the high-level tank a flow meter is inserted in series in the circuit, followed by a electromechanical valve to start the filling. To ensure hydraulic resistance a zone of strong constriction (5) is placed between the valve and the lower end of the flexible tube. The device is completed by four digital measurement chains. The first two measure the hydrodynamical variables: pressure and flow rate. The other two measure the tube diameter in two different directions at the same location, yielding the small and large axis of the section.

Measurements of flow were carried out with a flow-meter (Digiflow DFS 3W), and pressure measurements with a differential membrane sensor (Sedme-Thomson FAS 63) which measures the pressure difference between the interior of the pipe and atmospheric pressure. Such a pressure captor is characterized by a very small flow rate into the device as the membrane deforms. To measure the tube area we used one of two methods: a laser device or an Keyence ombroscopy apparatus measuring the apparent diameter. The laser device projects a very thin laser sheet on the flexible tube, and the image is recorded with a high-definition camera (Adimec MX12p – 60 images/s). The tube area is computed by numerical integration of the image shape. The ombroscopy apparatus sends a laser sheet over an receptor; the shadow zone delimited by the tube shape defines the apparent diameter. With two perpendicular diameters we can compute the tube area.

In the static configuration (no flow), we thus directly have the transmural pressure and the cross-section area, from which we obtain the tube law. If p is the pressure inside the tube and p_{ext} the pressure outside, the transmural pressure $p - p_{\text{ext}}$ is related to the tube area A by the tube law

$$p = f(A/A_0) + p_{\text{ext}} \tag{2.1}$$

where A_0 is an arbitrary reference area. In the present setup, p_{ext} is atmospheric pressure. Its variations are negligible and we thus shift the origin of the pressure axis so that $p_{\text{ext}} = 0$ in what follows. We measure f by a series of experiments where the tube is filled with air at various pressures. Measurements are made far enough from the walls to avoid the effect of longitudinal tension described below. The result is

https://doi.org/10.1017/S0022112003005834 Published online by Cambridge University Press

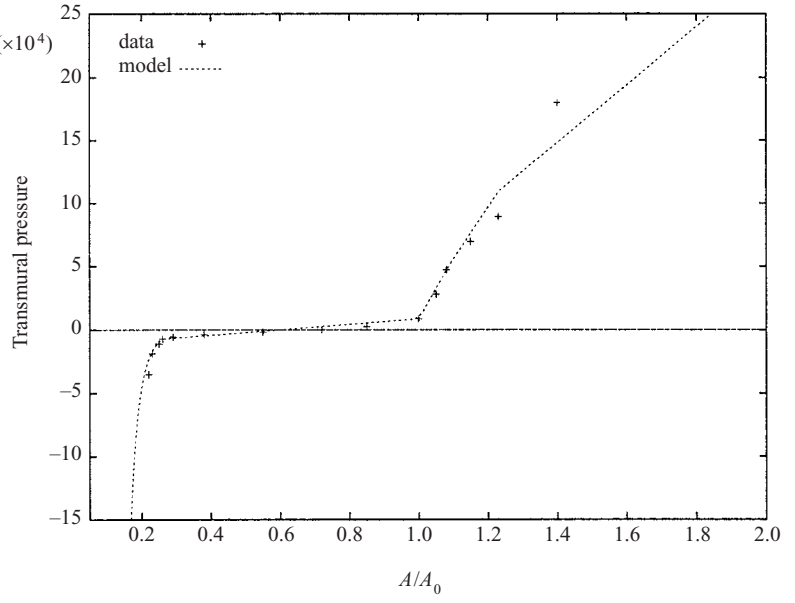


FIGURE 2. The experimentally measured tube law.

shown in figure 2. We also measured the longitudinal tension T of the tube before each filling experiment, using the same bench equipped with a dynamometer. In the dynamical configuration each pressure sensor is connected to the same acquisition chart which records the temporal signal of pressure flow. To summarize we have the possibility of making synchronous data acquisitions for complete cycles of draining and of filling.

3. Collapsible tube model and numerical predictions

We assume an unsteady, incompressible one-dimensional flow through a collapsible tube. The length scale for the variation of tube shape, velocity and pressure is large compared to the diameter of the tube. This assumption may fail in some cases, for instance near the ends of the tube where it is attached to rigid pipes. However these regions are small and the simplification is so useful that it is difficult to consider an alternative. This also means that transverse variations of pressure are neglected.

Therefore we consider the flow as one-dimensional: the pressure $p(x,t)$ and the velocity $u(x,t)$ are uniform over each cross-section. $A(x,t)$ is the area of the tube cross-section. Longitudinal non-uniformities in the tube shape are represented by gradients of the area $A(x,t)$. The governing equations for the fluid flow are the conservation of mass (Shapiro 1977)

$$\frac{\partial A}{\partial t} + \frac{\partial}{\partial x}(AU) = 0, \tag{3.1}$$

and conservation of momentum

$$\rho\frac{\partial U}{\partial t} + \rho U\frac{\partial U}{\partial x} = -\frac{\partial p_i}{\partial x} - \rho g - f_v. \tag{3.2}$$

https://doi.org/10.1017/S0022112003005834 Published online by Cambridge University Press

The momentum loss due to viscous effects is included in f_v. The one-dimensional model is derived from the Navier-Stokes equations integrated over a portion $\mathscr{P}$ of the tube bounded by two longitudinal sections $\mathscr{S}(x^* - dx/2)$ and $\mathscr{S}(x^* + dx/2)$ in the limit $dx \to 0$. The viscous term can be written

$$\int_{\mathscr{P}} \Delta u_x = \int_{\partial\mathscr{P}} \nabla u_x \cdot \boldsymbol{n} = -\int_{\mathscr{S}^-} \frac{\partial u_x}{\partial x} + \int_{\mathscr{S}^+} \frac{\partial u_x}{\partial x} + \int_{wall} \nabla u_x \cdot \boldsymbol{n}.$$

With the assumption that viscous effects are relevant only close to the wall boundary we assume that the function f_v is equal to $\int_{wall} \nabla u_x \cdot \boldsymbol{n}$. This function depends on the precise flow condition (Cancelli & Pedley 1985). For example, for laminar flow (Reynolds number less than 4000) and $A > A_0$ the momentum loss is $f_v = 8\pi\nu A^{-1}U$. For laminar flow and $A < A_0$ we have $f_v = 8\pi\nu A_0 A^{-2}U$ for an elliptical tube (Wild, Pedley & Riley 1977). This the last expression diverges for $A \to 0$. Our approach is to use a semi-analytical expression given by Ribreau, Naili & Langlet (1994), based on thin-shell theory and including some three-dimensional characteristics using a simple polynomial function $\mathscr{F}$. We define f_v as

$$f_v(A, U; \nu, A_0) = \mathscr{F}(A/A_0)\frac{\pi\nu U}{8A} \tag{3.3}$$

where $\mathscr{F} = 64$ for $A > A_0$, $\mathscr{F}(A/A_0) = a_0 + a_1 A/A_0 + a_2(A/A_0)^2 + a_3(A/A_0)^3$ for $A_l < A < A_0$ and $\mathscr{F} = fc$ for $A < A_l$. The value of A_l is computed from the osculation pressure $f(A_l/A_0)$ when contacts occurs along a straight line. The coefficients $\{fc, A_l/A_0, a_0, a_1, a_2, a_3\}$ are given by Ribreau *et al.* (1994) for different values of initial ellipticity. For our case, the value of initial ellipticity is 1, and the coefficients $\{31.92, 0.2095, -0.9128, 9.3479, -12.9856, 5.5503\}$.

The mechanical characteristics of the tube are described in a first approximation by the experimental tube law (2.1). However this description causes problems, because it allows sharp discontinuities of the tube area. For instance, if the transmural pressure at tube entry is non-zero, and the tube is attached so its area at $z = 0$ is A_0, there is a contradiction between the tube law and the attached area. Discontinuous solutions arise. To prevent this effect, we introduce a regularization term, the tension term $-T/R$. This term represents the Laplace law pressure which arises from a longitudinal curvature $1/R$:

$$p = f(A/A_0) - T/R. \tag{3.4}$$

where f is the experimental filling law. We assume a circular cross-section of radius $r = \sqrt{A/\pi}$, and

$$\frac{1}{R} = \frac{\partial^2 r}{\partial x^2}\left[1 + \left(\frac{\partial r}{\partial x}\right)^2\right]^{-3/2} \tag{3.5}$$

which we approximate by

$$\frac{1}{R} = \frac{1}{2\sqrt{\pi A_0}}\frac{\partial^2 A}{\partial x^2}. \tag{3.6}$$

These approximations for the curvature cease to be valid when the tube section ceases to be circular, as happens when the tube collapses. So why use model (3.4)–(3.6) for the longitudinal tension rather than no longitudinal tension term at all? Because the model without this terms admits discontinuous solutions, akin to shocks in gas dynamics. For instance the solution does not match the attachments smoothly but

https://doi.org/10.1017/S0022112003005834 Published online by Cambridge University Press

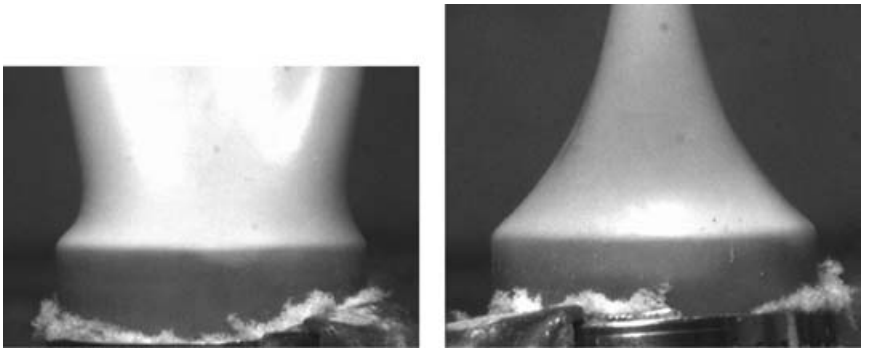


FIGURE 3. Two orthogonal views of the initial state near the lower end of the flexible tube.

discontinuously. The mathematical advantage of (3.4)–(3.6) is that they regularize these shocks, giving them a finite thickness as observed experimentally.

We use for T the value measured prior to the experiment, thus neglecting any variation as the tube deforms during the filling process, following the experimental study of McClurken *et al.* (1981).

The boundary conditions at the top of the tube ($x = L$) are $A(L) = A_1$ where A_1 is the external cross-section area of the rigid pipe, and $U(L) = 0$. At the bottom of the tube $A(0) = A_1$ while for U and p two approaches were used: (*a*) an imposed flow rate $A_1U(0) = Q(t)$ where $Q(t)$ is determined as discussed below and $A(0) = A_1$; (*b*) the flexible tube is coupled to a model of the hydraulic circuit. To model the upstream circuit, we introduce the mechanical properties of the rigid part of the system: the pressure drop across the rigid tube will be modelled by a resistive and an inertial term. The main contribution to the resistive term is classically taken proportional to the squared flow rate, and the inertial one as an effective length times the fluid acceleration:

$$p(0,t) = p_R - \rho L_{\text{circuit}} \frac{\mathrm{d}U}{\mathrm{d}t}(0,t) - kL_{\text{circuit}}\rho U^2(0,t) \tag{3.7}$$

where $p_R = \rho g h_1$ is the reference pressure or the hydrostatic pressure difference between the free surface of the feed reservoir at height h_1 and the origin of the flexible tube, L_{circuit} is the equivalent length, and k is a friction coefficient with dimensions of length and depends in a complex way on the shape of the hydraulic circuit. The circuit contains a portion of narrow diameter designed to stabilize the flow rate.

The initial state of the tube is prepared by first filling it and making sure that no air remains. It is then drained into the lower reservoir at height h_2 so that the transmural pressure at the origin is negative and the tube is completely collapsed. The valve is then closed and the tube is connected to the upper reservoir at height h_1. The initial condition is thus a uniform negative pressure $p(x,0) = \rho g(h_2 - x)$ and a static profile $A(x,0)$ which is the solution of equation (3.4) with imposed pressure.

4. Results

Figure 3 shows the initial state near the lower end of the flexible tube. It is strongly collapsed by the negative pressure and the deformation is clearly not axisymmetric. The results of pressure and flow rate measurements as well as numerical predictions

https://doi.org/10.1017/S0022112003005834 Published online by Cambridge University Press

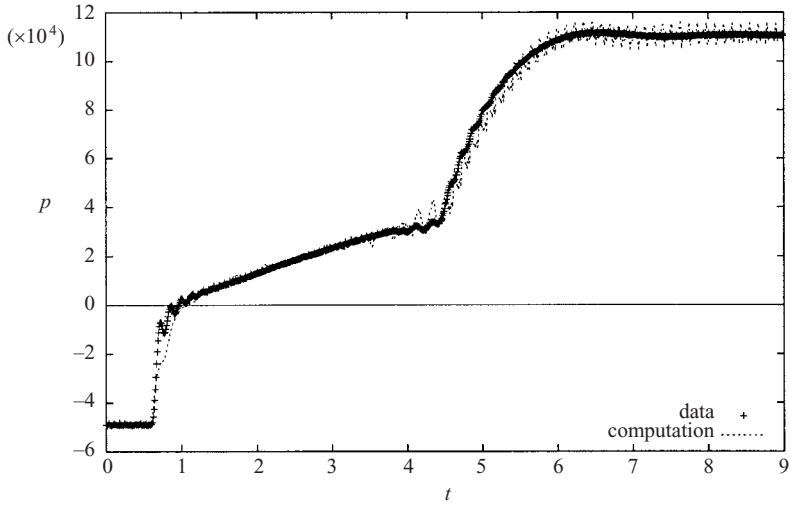


FIGURE 4. Results of pressure measurements and of computations.

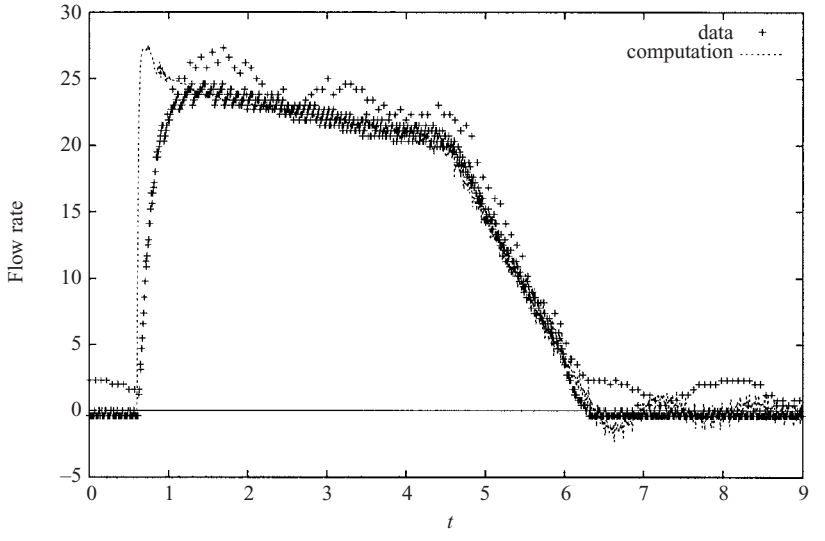


FIGURE 5. Results of flow rate measurements and of computations.

for a typical experiment are shown on figures 4 and 5. In our parameter range the filling process occurs in three phases, each with different dominant phenomena.

(i) Initial transient: a rapid increase of the flow rate, together with a jump of the pressure from p_{init} to zero. Waves propagate along the tube with a short period. The jump to approximately zero pressure may be explained by the simple model given below.

(ii) Quasi-steady filling: the quasi-constant flow rate measured at the tube entry marks the beginning of the second phase. The pressure increases more slowly and approximately linearly. The flow rate decreases slowly during this phase.

https://doi.org/10.1017/S0022112003005834 Published online by Cambridge University Press

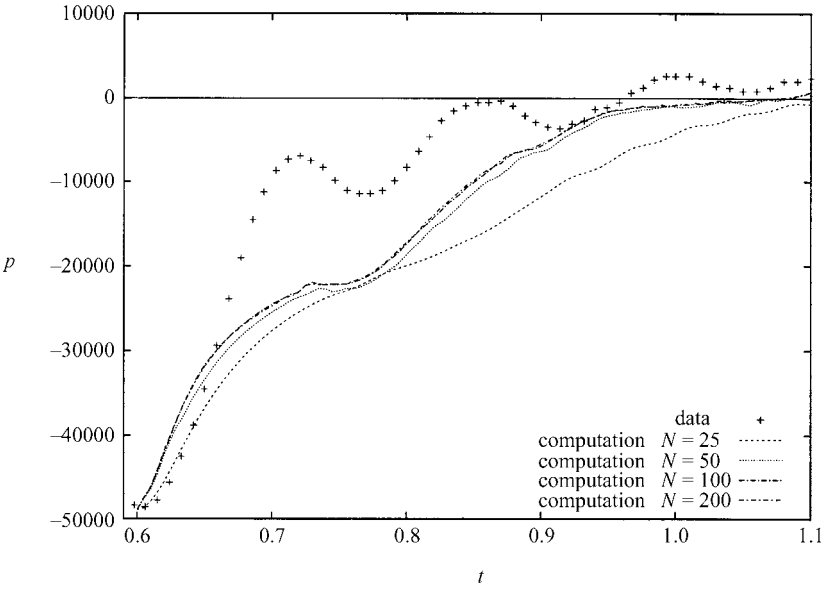


FIGURE 6. Detail of the initial transient phase.

L	$\rho g h_1$	$\rho g h_2$	T	A_0	A_1	L_{circuit}	k	N
40.6	110412	−23436.5	194000	3.56	2.75	150	5.5	200

TABLE 1. Parameters used in the computation (see text).

(iii) Final stage: the flow rate decreases rapidly to near zero. The irregular bumps in the flow rate data are artifacts of the flow metering procedure. The pressure has a clear change of slope and convergences slowly to the reservoir pressure $\rho g h_2$. Our computations are performed by discretizing the tube equations using a standard Mac Cormack scheme. Convergence was observed when varying the number of grid points from $N = 25$ to 200 (figure 6). The result of these computations, using the model hydraulic circuit is shown on figures 4 and 5. The determination of model parameters was as follows. The model hydraulic circuit (3.7) has two parameters. To determine L_{circuit} we performed an independent experiment on the same bench with a rigid tube instead of the flexible one, which yielded $L_{\text{circuit}} = 150$. Due to the difficulty of precisely reproducing the same experimental conditions the resistance parameter k was fit by adjusting the flow rate in the quasi-steady filling phase. The parameters L, A_1, h_1, h_2 and T are directly measured and the values shown in table 1. The results are very sensitive to small variations of A_1, h_1 and h_2 while moderate variations of T have little effect.

The tube law (3.4) is a piecewise interpolation from the measured values as shown on figure 2. The results of the fit are very sensitive to the tube law. (In particular, we found that an initially erroneous tube law, obtained from a different procedure for the measurement of A, gave markedly worse results.)

The correspondence between measurements and computations is very good except in some aspects. For the initial transient phase, the computed pressure does not rise

https://doi.org/10.1017/S0022112003005834 Published online by Cambridge University Press

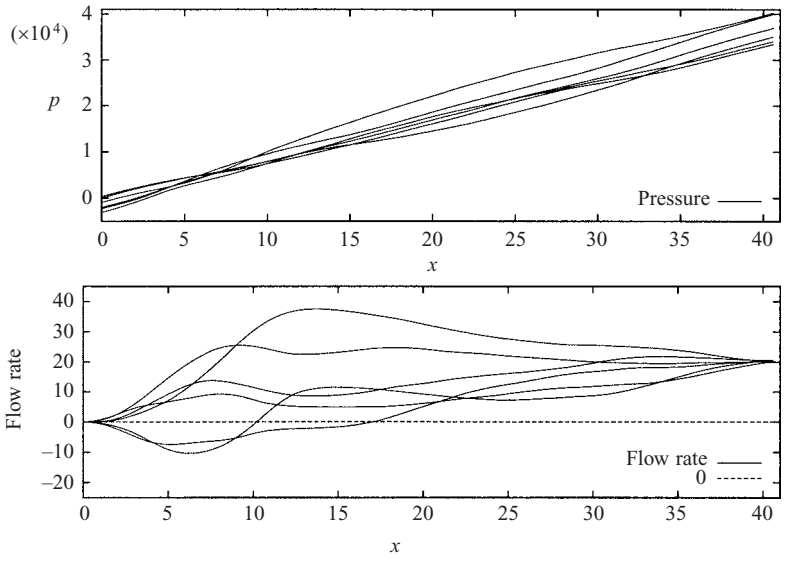


FIGURE 7. Two superposed plots at time $t = 4.35$ with an interval of 0.02 s. Origin of the time axis is as on the previous figures. The x- axis is reversed, the tube bottom is on the right. (*a*) Pressure (*b*) flow rate. The plots show waves propagating rapidly along the tube axis and reflecting near the top of the tube. These waves create small variations of the tube cross-section but large variations in pressure and velocity, which can also be seen on figure 4.

exactly as in the experiments as shown on figure 6. Varying L_{circuit} does not improve the agreement. It is likely instead that three-dimensional effects play a role. There is also a strong oscillation of the pressure at the end of the quasi-steady filling phase. Our computations show that waves of very large amplitude travel back and forth along the tube at this stage (see figure 7). The pressure waves are superimposed on a strong hydrostatic pressure gradient and are seen to travel to the right in this case. The flow rate shows waves trapped near the top of the tube (on the left) as well as waves reaching the bottom of the tube and reflecting there. The flow rate varies very little at the bottom, which shows that the boundary condition mainly fixes the flow rate. The flow rate shows very good agreement with experiments. However the experimental rise seems slower than the computed one. This is due to the inertia of the flowmeter, a feature observed independently.

We changed the boundary conditions at the bottom of the tube to impose an artificial flow rate signal that closely mimics the real inflow. As shown on figure 8 the artificial flow rate rises discontinuously (we expected a much faster rise than seen in the flowmeter data because of the inertia of the flowmeter) then decreases with two linear slopes. It is then blocked to zero (which filters some oscillations of the flow rate around zero occurring when the tube slowly reaches equilibrium). The boundary condition is then $q(0, t) = q_{synth}(t)$ and p is left free. The result, shown on figure 9 is very similar to that using the hydraulic circuit. There are however larger oscillations of pressure at the end of the experiment, probably due to the blocking of the flow rate at entry in the final phase. We conjecture that these oscillations are caused by the tube law we have adopted. This law conserves the elastic energy, and any viscous dissipation in the flow is also small for long wavelengths. Adding a viscoelastic term to the tube wall (2.1) would improve the results.

https://doi.org/10.1017/S0022112003005834 Published online by Cambridge University Press

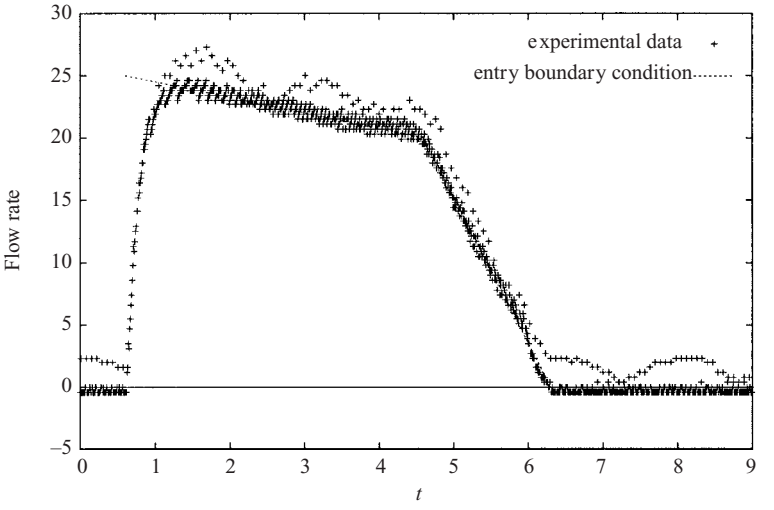


FIGURE 8. The artificial signal used in modelling the flow entry. The signal is piecewise linear and matches closely the flow rate measurements.

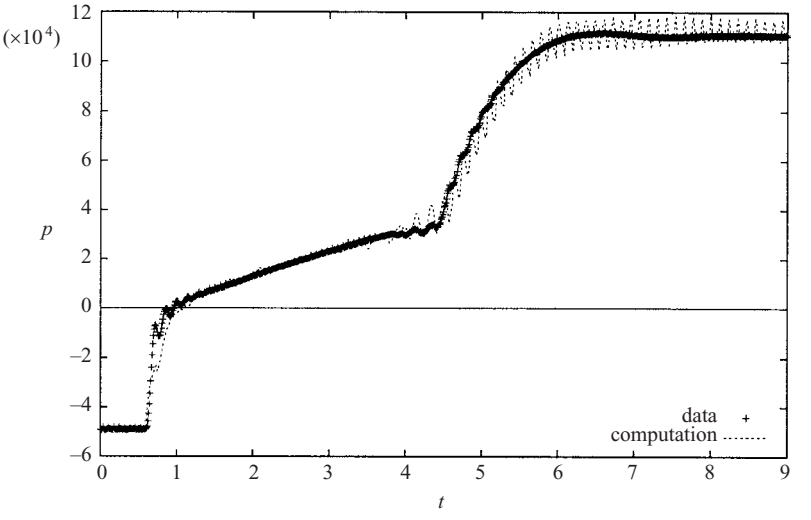


FIGURE 9. Pressure measurements compared to computations with the artificial flow entry. This setup leads to oscillations of the computed pressure and indicates that the direct forcing of the pressure in the boundary condition is not a well-posed problem.

In a similar way we attempted to impose the pressure at entry. The boundary condition is $p(0, t) = p_{exp}(t)$ and q is left free. In this case we apply the experimentally recorded pressure at entry $p_{exp}(t)$ shown on figure 4. The resulting flow rate is shown on figure 10. Very wide variations of the calculated flow rate are seen. This indicates a very large sensitivity of the system to errors in the pressure or in parameters. The direct forcing of the pressure in the boundary condition is not a well-posed problem, and coupling with the hydraulic circuit appears necessary.

https://doi.org/10.1017/S0022112003005834 Published online by Cambridge University Press

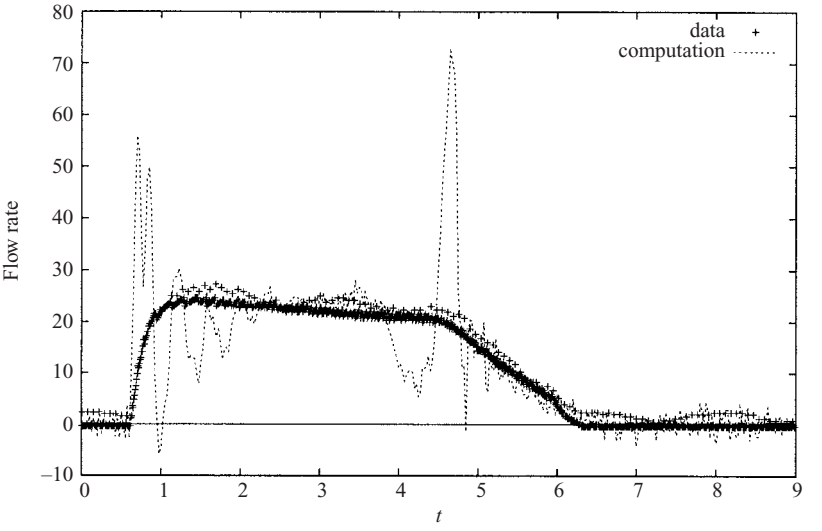


FIGURE 10. Flow rate measurements compared to computations with the experimental pressure imposed at entry. Very large fluctuations are seen in the computed flow rates, which hints that the imposed pressure is not adequately matched to the tube parameters of the model.

5. Conclusions

Our experimental results show that in the range of parameters considered, and in particular with the kind of tube law we choose, the filling of the tube occurs in three stages, one being a quasi-steady filling. It is likely that this type of behaviour applies to external veins in quasi-contact with the atmosphere and not to internal veins which have a different tube law. Our study also shows that a one-dimensional collapsible tube model describes this behaviour well, both quantitatively and qualitatively. No particular stability or convergence problems are found. However the boundary conditions play a very important role. The boundary conditions that we tested in this study are adequate, but others may cause difficulty. For instance imposing at the tube entry a flow rate not consistent with the tube parameters may lead to unphysical fluctuations.

We see a clear deviation from experiment in the initial transient for which we do not have a clear explanation. The flow rate measurements on this time scale are obscured by the flowmeter bandwidth inertia and the tube area varies very little during the transient. The observed waves are the result of the interaction of fluid mechanics with a complex three-dimensional tube structure which cannot be attained by the present model.

However the predictions of the model in the subsequent stages are not significantly affected by the initial transient. It is likely that the collapsible tube model would also yield quantitatively correct predictions for biomedical applications.

The contribution on experimental setup of Pascal Guesdon (LBHP) is gratefully acknowledged.

REFERENCES

CANCELLI, C. & PEDLEY, T. J. 1985 A separated flow model for collapsible tube oscillations. *J. Fluid Mech.* **157**, 375–404.

https://doi.org/10.1017/S0022112003005834 Published online by Cambridge University Press

Conrad, W. A. 1969 Pressure-flow relationships in collapsible tubes. *IEEE Trans. Biomed. Engng* **16**, 284–295.

Elad, D., Kamm, R. D. & Shapiro, A. H. 1987 Choking phenomena in a lung like model. *Trans. ASME: J. Biomech. Engng* **109**, 1–9.

Flaherty, J. E., Keller, J. B. & Rubinow, S. I. 1972 Post buckling behavior of elastic tubes and rings with opposite sides in contact. *SIAM J. Appl. Math* **23**, 446–455.

Fung, Y. C. 1993 *Biomechanics: Mechanical Properties of Living Tissues*. Springer.

Griffiths, D. J. 1971 Hydrodynamics of male micturation. I. theory of steady flow through elastic walled tubes. *Med. Biol. Engng* **9**, 581–588.

Holt, J. P. 1969 Flow through collapsible tubes and through in situ veins. *IEEE Trans. Biomed. Engng* **16**, 274–283.

Ikeda, T. & Matsuzaki, Y. 1999 A one-dimensional unsteady separable and reattachable flow model for collapsible tube-flow analysis. *Trans. ASME: J. Biomech. Engng* **121**, 153–159.

Jan, D. L., Kamm, R. D. & Shapiro, A. H. 1983 Filling of partially collapsed compliant tube. *Trans. ASME: J. Biomech. Engng* **105**, 12–18.

Jensen, O. E. 1990 Instabilities of flow in a collapsed tube. *J. Fluid Mech.* **220**, 623–659.

Jensen, O. E. 1992 Chaotic oscillations in a simple collapsible-tube model. *Trans. ASME: J. Biomech. Engng* **114**, 55–59.

Jensen, O. E. & Pedley, T. J. 1989 The existence of steady flow in a collapsed tube. *J. Fluid Mech.* **206**, 339–374.

Kamm, R. D. 1982 Bioengineering studies of periodic external compression as prophylaxis against deep vein thrombosis – Part I: Numerical studies. *Trans. ASME: J. Biomech. Engng* **104**, 87–95.

Kamm, R. D. & Pedley, T. J. 1989 Flow in collapsible tube: a brief review. *Trans. ASME: J. Biomech. Engng* **111**, 177–179.

Kamm, R. D. & Shapiro, A. H. 1979 Unsteady flow in a collapsible tube subjected to external pressure of body forces. *J. Fluid Mech.* **95**, 1–78.

Matsuzaki, Y. & Fung, Y. C. 1976 On separation of a divergent flow at moderate Reynolds numbers. *J. Appl. Mech.* **43**, 227–231.

Matsuzaki, Y. & Fung, Y. C. 1977 Unsteady fluid dynamic forces on a simply-supported circular cylinder of finite length conveying a flow, with applications to stability analysis. *J. Sound Vib.* **54**, 317–330.

Matsuzaki, Y. & Matsumoto, T. 1989 Flow in a two-dimensional collapsible channel with rigid inlet and outlet. *Trans. ASME: J. Biomech. Engng* **111**, 180–184.

McClurken, M. E., Kececioglu, I., Kamm, R. D. & Shapiro, A. H. 1981 Steady, supercritical flow in collapsible tubes. Part 2. Theoretical studies. *J. Fluid Mech.* **109**, 391–415.

Olson, D. A., Kamm, R. D. & Shapiro, A. H. 1982 Bioengineering studies of periodic external compression as prophylaxis against deep vein thrombosis – Part II: Experimental studies on a simulated leg. *Trans. ASME: J. Biomech. Engng* **104**, 96–104.

Pedley, T. J. 1980 *The Fluid Mechanics of Large Blood Vessels*. Cambridge University Press, London.

Pedley, T. J. 1992 Longitudinal tension variation in collapsible channels: A new mechanism for the breakdown of steady flow. *Trans. ASME: J. Biomech. Engng* **114**, 60–67.

Ribreau, C., Naili, S. & Langlet, A. 1994 Head losses in smooth pipes obtained from collapsed tubes. *J. Fluids Struc.* **8**, 183–200.

Shapiro, A. H. 1977 Steady flow in collapsible tubes. *Trans. ASME: J. Biomech. Engng* **99**, 126–147.

Wild, R., Pedley, T. J. & Riley, D. S. 1977 Viscous flow in collapsible tubes of slowly-varying elliptical cross-section. *J. Fluid Mech.* **81**, 273–294.

Young, D. F. & Tsai, F. Y. 1975 Flow characterists in models of arterial stenosis. I. Steady flow. *J. Biomech.* **6**, 395–410.

https://doi.org/10.1017/S0022112003005834 Published online by Cambridge University Press